Research Square

Preprints are preliminary reports that have not undergone peer review.
They should not be considered conclusive, used to inform clinical practice,
or referenced by the media as validated information.

Genome-Wide Analysis and Functional Characterization of the NRT1 Gene Family in Grapevine (Vitis vinifera L.) Reveals Roles of VvNRT1.19 and VvNRT1.47 in Salt Stress and Nitrogen Response

Chen Zhou
Yangzhou University
Yingchun Chen
Shandong Academy of Agricultural Sciences
Kai Liu
Shandong Academy of Agricultural Sciences
Xiujie Li
Shandong Academy of Agricultural Sciences
Xuehui Zhao
Weifang University
Bo Li
Shandong Academy of Agricultural Sciences
Li Liu
151538715690163.com

Shandong Academy of Agricultural Sciences
Zhaosen Xie
Yangzhou University

Research Article

Keywords: Genome-wide analysis, Nitrate Transporters, Grapevine, Gene expression, Gene function

Posted Date: March 19th, 2026

DOI: https://doi.org/10.21203/rs.3.rs-8769993/v1

License: This work is licensed under a Creative Commons Attribution 4.0 International License.
Read Full License

Additional Declarations: No competing interests reported.

Abstract

Background

The *NRT1* (nitrate transporter 1) family is referred to as the *NPF* (nitrate/peptide transporter family). It constitutes the largest and most functionally diverse group of nitrate transporters in plants and plays an essential role in nitrate translocation and allocation. These are fundamental to plant growth, development, and stress adaptation. However, a comprehensive genome-wide characterization of this family in grapevine (*Vitis vinifera* L.) remains unexplored.

Results

A total of 65 *NRT1* genes were identified in the grapevine genome and phylogenetically classified into five distinct clades. Their physicochemical properties, as well as gene and protein structural features, were analyzed in detail. Homology analyses revealed that both segmental and tandem duplication events played major roles in driving the expansion of the *VvNRT1* gene family. In addition, analysis of tissue-specific expression patterns and cis-regulatory elements suggested that *VvNRT1* genes participated in the regulation of grapevine development and adaptive responses to diverse environmental stresses. Nitrate treatment and salt stress induced the expression of multiple *VvNRT1s*, among which *VvNRT1.19* and *VvNRT1.47* exhibited the most pronounced transcriptional upregulation. The expression levels of these two genes were positively associated with nitrogen uptake capacity and salt tolerance in grapevine. Furthermore, heterologous overexpression of *VvNRT1.19* and *VvNRT1.47* in *Arabidopsis* significantly enhanced nitrogen use efficiency and salt tolerance, thereby promoting plant growth and improving stress resistance.

Conclusion

This study presents a comprehensive characterization of the *VvNRT1* gene family and provides insights into its evolutionary history in grapevine. *VvNRT1.19* and *VvNRT1.47* are proposed to function as positive regulators of plant responses to stress. Collectively, these findings establish a solid foundation for future functional investigations of *NRT1* genes and highlight their potential roles in improving nitrogen regulation and salt stress tolerance in grapevine.

Background

Nitrogen is an essential mineral element required for plant growth and development and can be involved in the synthesis of key biological molecules, including proteins, nucleic acids, chlorophyll, and hormones [1]. The efficiency of nitrogen absorption, transport, and assimilation directly determines plant growth rate, yield formation, and quality regulation. Nitrate (NO_3^-) and ammonium (NH_4^+) are the major inorganic nitrogen (N) sources available to plants. Owing to its high mobility in soil and ready

accessibility to roots, NO_3^- is the predominant nitrogen form taken up by most plant species [2]. NO_3^- uptake mainly occurs in plant roots and is mediated by nitrate transporter (NRT) proteins, which are widely recognized as essential for N acquisition in plants. Transmembrane NO_3^- transport depends on the precise regulation of NRTs, which are classified into three families, *NRT1*, *NRT2*, and *NRT3*, according to their functional characteristics and sequence homology. Among these families, *NRT1*, referred to as the Nitrate Peptide Transporter Family (NPF), contains the largest number of members and exhibits the broadest functional diversity [3]. Therefore, it has become the central focus of recent plant nitrogen metabolism research.

NRT proteins are pivotal for nitrate transport and distribution, with their primary function being the mediation of root NO_3^- uptake. Based on the differences in external nitrate concentrations, *NRT* family members are divided into two transport systems: the Low-Affinity Transport System (LATS) and the High-Affinity Transport System (HATS). Under low NO_3^- conditions, typically below 1 mM, NO_3^- uptake is dominated by HATS, which is mainly mediated by the NRT2 family. Under high NO_3^- concentrations, generally above 1 mM, LATS dominated by the NRT1 family takes precedence [4–5]. However, certain NRT1 members (e.g., *NRT1.1* (*AtNPF6.3*) in *Arabidopsis thaliana*) exhibit “dual-affinity” characteristics, enabling roots to absorb NO_3^- from the soil while also functioning as NO_3^- sensors that coordinate N uptake and carbon metabolism through the regulation of downstream gene expression [6]. *AtNPF7.2* (*NRT1.8*) is specifically localized in xylem parenchyma cells and is responsible for reloading NO_3^- from xylem sap, thereby regulating NO_3^- allocation to shoots and influencing leaf photosynthesis and nitrogen remobilization [7]. Furthermore, *AtNPF4.6* participates in drought stress responses by transporting abscisic acid (ABA), whereas *AtNPF5.5* regulates storage substance accumulation during seed development, highlighting the central role of the NRT1 family within the “nitrogen metabolism-growth and development-stress adaptation” network [8–9]. With the development of genome sequencing technologies, studies on the NRT1 family have expanded from model plants to diverse crops and economically important species. In rice, natural variation in *OsNRT1.1B* is associated with nitrogen use efficiency, with cultivars containing specific alleles exhibiting higher yields under low-nitrogen conditions [10]. *OsNPF6.5* influences grain protein content by regulating root NO_3^- uptake and N allocation to panicles [11]. In maize, *ZmNRT1.1* expression is induced by low-nitrogen stress, with overexpression significantly increasing plant biomass in N-deficient soils. This demonstrates the breeding potential of this gene family for N-efficient crops [12]. In fruit trees, *MdNPF6.5* functions as a key low-nitrogen-inducible nitrate transporter that plays a critical role in significantly enhancing apple tolerance under low-nitrogen conditions [13]. Collectively, these studies indicate that the NRT1 family exhibits both functional conservation, such as core nitrate transport activity across plant lineages, and species-specific characteristics shaped by evolutionary history.

Salt stress is a major abiotic stressor that constrains global crop production and severely disrupts N metabolic balance. Numerous studies have demonstrated that salt stress markedly inhibits plant NO_3^- uptake and assimilation capacity, leading to a decline in leaf nitrate content. In peanut, salt stress

reduces NO_3^- accumulation in leaves, with the inhibitory effect intensifying as the salt concentration increases, a response closely associated with the suppressed expression of nitrate transporters [14]. Similarly, in rice, treatment with 0.3% NaCl significantly decreases NO_3^- content and the activities of nitrate reductase (NR), glutamine synthetase (GS), and NADH-dependent glutamate synthase (NADH-GOGAT) in both roots and leaves, while increasing ammonium accumulation and the activities of glutamate dehydrogenase (GDH) and aspartate aminotransferase (AST). These changes indicate a metabolic shift from the NO_3^- assimilation pathway to alternative nitrogen metabolic routes under salt stress conditions [15]. Under salt stress, NRT1 family proteins enhance plant adaptability through multiple mechanisms, including the maintenance of N uptake, regulation of ion homeostasis, participation in signal transduction, and facilitation of root architecture remodeling. For instance, in *Suaeda salsa* under high-salinity and low-N conditions, N uptake is promoted by the induction of SsNRT2.1/2.5 expression acting in concert with NRT1, along with the activation of plasma membrane H^+-ATPases that drive proton gradient–dependent active NO_3^- transport [16–17]. In *Arabidopsis*, *NRT1.5* (*NPF7.3*) functions as an H^+/K^+ antiporter that facilitates K^+ transport to shoots, and the *NRT1.5* (*lks2*) knockout mutant exhibits leaf chlorosis under salt stress, indicating its role in alleviating Na^+ toxicity by maintaining K^+ homeostasis [18]. In rice, *NRT1.1* (*OsNRT1.1B*) acts as a NO_3^- sensor and activates transcription factors such as *ANR1* and *NLP7* to regulate downstream gene expression [19]. Ectomycorrhizal fungi, such as *Paxillus involutus*, mitigate salt stress–induced nitrate efflux by activating host poplar genes PcNRT1.1/1.2 and *PcHA4*, lowering rhizosphere pH, and promoting H^+-ATPase activity [20].

Grapevine (*Vitis vinifera* L.) is one of the world's most economically important fruit crops and is characterized by a long growth cycle and complex synchrony of organ development, resulting in pronounced stage-specific N demands. High nitrogen availability is required at budburst to support shoot growth, whereas insufficient nitrogen supply from flowering to fruit enlargement leads to reduced fruit set, and excessive N input during ripening inhibits fruit coloration and flavor compound accumulation[21–22]. With ongoing changes in the global ecological environment, grapevine growth is increasingly affected by environmental pressures, s uch as salt stress. Our previous research indicated that salt stress adversely affected N absorption and assimilation in grapevine and ultimately constrained plant growth [23]. Therefore, elucidating the molecular mechanisms underlying nitrogen uptake and transport in grapevine is of practical significance for N management and fruit quality optimization. The recent completion of grapevine whole-genome sequencing projects, including the PN40024 reference genome and high-quality assemblies such as the CHR_T2T2 telomere-to-telomere genome, can provide crucial support for functional gene mining [24]. However, research on the grapevine *NRT1* gene family remains limited [25]. Early studies primarily predicted a small number of potential members through homology-based sequence alignment and focused mainly on expression pattern analyses of genes related to root nitrate uptake, such as *VvNRT1.1* [26]. Core questions regarding the genome-wide identification of family members, phylogenetic relationships, gene structural variations, tissue-specific expression patterns, and associations with stress responses remain largely unresolved. To address

these issues, the present study performed a genome-wide analysis and identified 65 full-length *NRT1* genes in grapevine. Using a multifaceted bioinformatic framework, this study characterized the physicochemical properties, gene and protein architectures, chromosomal distributions, phylogenetic relationships, and tissue-specific expression patterns of the identified genes. These findings advance our understanding of the functional landscape of the grapevine *NRT1* gene family and highlight its potential involvement in salt stress response mechanisms.

Results

VvNRT1s gene identification

To identify potential NRT1 homologs in the grapevine genome (PN_T2T2) [27], *Arabidopsis* NRT1 protein sequences were used as queries for BLASTP searches. This initial screening retrieved approximately 80 candidate proteins. Subsequent validation using the SMART and NCBI-CDD databases confirmed the presence of characteristic MFS and extensin domains. After this filtering step, 65 *VvNRT1* proteins were identified (Fig. S1), representing a number higher than that reported in Arabidopsis. These genes were systematically designated *VvNRT1.1–VvNRT1.65* according to their linear positions on the chromosomes.

The predicted molecular weights of the 65 *VvNRT1* proteins ranged from 10.6 kDa for *VvNRT1.40* to 162.42 kDa for *VvNRT1.63*. Consistent with this variation, the protein lengths differed markedly, spanning from 96 amino acids (*VvNRT1.40*) to 1466 amino acids (*VvNRT1.63*). In addition, the theoretical isoelectric points of these proteins varied from 4.82 for *VvNRT1.55* to 9.8 for *VvNRT1.6* (Table 1).

Table 1
Characteristics of NRT1s in Grapevine (*Vitis vinifera* L.).

Gene name	Gene ID	Chromosome location	Exon	Size (amino acids)	MW (kDa)	pI
VvNRT1.1	VitviT2T_000270	chr1:3035085 – 308496	4	583	64.50	8.8
VvNRT1.2	VitviT2T_000553	chr1:6408849–6416804	5	586	64.61	5.47
VvNRT1.3	VitviT2T_000867	chr1:10897334–10901324	4	619	68.52	8.73
VvNRT1.4	VitviT2T_000875	chr1:10997314–11001502	4	585	64.42	9.18
VvNRT1.5	VitviT2T_001641	chr1:27439472–27442560	4	640	70.83	9.01
VvNRT1.6	VitviT2T_002188	chr2:5135546–5146196	7	786	86.01	9.8
VvNRT1.7	VitviT2T_002412	chr2:8626578–8631608	4	591	65.58	6.36
VvNRT1.8	VitviT2T_002882	chr2:20036564–20037454	1	296	33.82	8.97
VvNRT1.9	VitviT2T_004646	chr4:2928810–2931535	4	589	65.19	6.1
VvNRT1.10	VitviT2T_004647	chr4:2933378–2935949	4	592	65.11	7.87
VvNRT1.11	VitviT2T_006768	chr5:9116491–9121269	4	592	65.81	9.22
VvNRT1.12	VitviT2T_007807	chr6:1599766–1602508	5	611	66.98	5.7
VvNRT1.13	VitviT2T_007840	chr6:1993924–1996770	3	534	60.21	8.78
VvNRT1.14	VitviT2T_007842	chr6:2057074–2064811	6	667	76.65	8.36
VvNRT1.15	VitviT2T_008029	chr6:4410373–4410825	1	150	16.85	8.82
VvNRT1.16	VitviT2T_008030	chr6:4427501–4430493	4	577	63.38	9.1
VvNRT1.17	VitviT2T_008032	chr6:4458253–4460909	4	577	63.46	8.97
VvNRT1.18	VitviT2T_008280	chr6:6896959–6901242	4	582	64.59	6.86
VvNRT1.19	VitviT2T_009857	chr7:7407053–7410478	4	597	66.78	9.05
VvNRT1.20	VitviT2T_009858	chr7:7415929–7419696	4	609	68.12	8.93
VvNRT1.21	VitviT2T_012005	chr8:12945007–12949683	4	599	66.23	9.08
VvNRT1.22	VitviT2T_012348	chr8:16570040–16573831	4	587	65.30	8.92

Gene name	Gene ID	Chromosome location	Exon	Size (amino acids)	MW (kDa)	pI
VvNRT1.23	VitviT2T_012404	chr8:17138913–17142492	4	568	64.06	9.08
VvNRT1.24	VitviT2T_012405	chr8:17144873–17147263	4	569	63.44	8.15
VvNRT1.25	VitviT2T_012415	chr8:17228720–17245294	5	444	50.42	8.72
VvNRT1.26	VitviT2T_013400	chr9:3797543–3801577	4	622	69.06	9.07
VvNRT1.27	VitviT2T_015272	chr10:8758372–8760963	5	596	65.70	8.45
VvNRT1.28	VitviT2T_016500	chr11:2931120–2933169	4	598	66.42	8.66
VvNRT1.29	VitviT2T_016501	chr11:2935712–2937182	4	276	31.13	9.62
VvNRT1.30	VitviT2T_016502	chr11:2937227–2937730	1	167	17.84	4.99
VvNRT1.31	VitviT2T_016649	chr11:4416724–4425469	7	623	68.53	8.89
VvNRT1.32	VitviT2T_016651	chr11:4443282–4446833	5	587	64.51	9.07
VvNRT1.33	VitviT2T_016652	chr11:4447461–4448228	3	143	15.54	9.12
VvNRT1.34	VitviT2T_017823	chr12:6204846–6208077	4	594	66.15	9.18
VvNRT1.35	VitviT2T_018872	chr12:24010632–24013783	5	607	66.81	8.83
VvNRT1.36	VitviT2T_019055	chr13:1289308–1293528	5	628	70.23	9.43
VvNRT1.37	VitviT2T_019317	chr13:3795593–3798375	4	597	67.00	8.93
VvNRT1.38	VitviT2T_020247	chr13:23151898–23154691	4	575	63.23	8.97
VvNRT1.39	VitviT2T_020250	chr13:23182256–23187154	3	499	56.11	9.43
VvNRT1.40	VitviT2T_020251	chr13:23189064–23189462	1	96	10.60	8.93

Gene name	Gene ID	Chromosome location	Exon	Size (amino acids)	MW (kDa)	pI
VvNRT1.41	VitviT2T_020253	chr13:23198483–23204010	3	538	59.28	8.86
VvNRT1.42	VitviT2T_020751	chr14:295133–297492	5	620	68.37	7.55
VvNRT1.43	VitviT2T_021566	chr14:13040883–13041776	3	169	19.08	8.95
VvNRT1.44	VitviT2T_021877	chr14:20772346–20774714	3	198	21.18	6.8
VvNRT1.45	VitviT2T_022515	chr14:28488931–28491946	4	533	59.81	8.9
VvNRT1.46	VitviT2T_022572	chr14:28916994–28979694	4	585	64.43	9.01
VvNRT1.47	VitviT2T_023196	chr15:12838567–12843593	5	604	67.47	8.48
VvNRT1.48	VitviT2T_023463	chr15:17551952–17554126	6	529	58.63	8.79
VvNRT1.49	VitviT2T_026074	chr17:6447730–6450309	4	577	64.05	9.31
VvNRT1.50	VitviT2T_026075	chr17:6451581–6454340	4	586	64.99	8.78
VvNRT1.51	VitviT2T_026076	chr17:6456777–6459464	4	586	64.56	9.22
VvNRT1.52	VitviT2T_026077	chr17:6463343–6465728	5	570	62.82	8.01
VvNRT1.53	VitviT2T_026078	chr17:6465936–6466590	3	132	13.98	6.25
VvNRT1.54	VitviT2T_026087	chr17:6540785–6543752	4	579	63.57	8.81
VvNRT1.55	VitviT2T_026703	chr17:16544148–16544727	2	141	15.37	4.82
VvNRT1.56	VitviT2T_027631	chr18:9572337–9575747	6	587	64.75	8.53
VvNRT1.57	VitviT2T_027795	chr18:11322484–11324487	5	617	68.27	8.34
VvNRT1.58	VitviT2T_027796	chr18:11327097–11329870	5	581	64.58	8.76

Gene name	Gene ID	Chromosome location	Exon	Size (amino acids)	MW (kDa)	pI
VvNRT1.59	VitviT2T_028874	chr18:30296518–30344687	6	1035	114.29	8.86
VvNRT1.60	VitviT2T_028876	chr18:30380900–30411853	4	894	99.07	8.77
VvNRT1.61	VitviT2T_028878	chr18:30435965–30446252	3	531	59.04	8.97
VvNRT1.62	VitviT2T_028880	chr18:30447236–30447676	1	146	16.50	7.74
VvNRT1.63	VitviT2T_028881	chr18:30468432–30497044	9	1466	162.42	6.8
VvNRT1.64	VitviT2T_028883	chr18:30527824–30544755	9	1139	126.20	6.98
VvNRT1.65	VitviT2T_029282	chr18:36195994–36199645	5	609	67.44	9.12

Phylogenetic and synteny analyses of VvNRT1s

To clarify the evolutionary and phylogenetic relationships, an unrooted phylogenetic tree was constructed using 32 AtNRT1 and 65 VvNRT1 protein sequences (Fig. 1a). The resulting topology grouped the NRT1 proteins into five primary clades (□–□). Group □ represented the largest clade, containing twenty-six members, whereas Groups □ and □ each comprised 17 proteins. In contrast, Groups □ and □ were much smaller, consisting of two and three proteins, respectively. Notably, this five-clade classification differed from the three-group pattern commonly reported for most other plant species.

The *VvNRT1* genes were unevenly distributed across the 16 grapevine chromosomes (Fig. 1b). Only one gene was located on chromosomes 5, 9, and 10, whereas chromosomes 4, 7, 12, and 15 each harbored two *VvNRT1* members. In contrast, most *VvNRT1* genes were preferentially clustered on chromosomes 6, 11, 13, 17, and 18. Among these, chromosome 18 contained the highest number of *VvNRT1* genes, suggesting a potentially prominent role for this chromosome in nitrate transport and metabolism in grapevine. To explore the evolutionary mechanisms underlying the expansion of the *VvNRT1* gene family, gene duplication events were analyzed. Based on sequence homology, 20 *VvNRT1* genes (30.77%) formed 10 segmental duplication pairs, whereas 42 *VvNRT1* genes (64.62%) formed 29 tadem duplication pairs (Fig. 1b and Table S2).

Conserved motif and gene structure analyses of VvNRT1s

The conserved protein motifs and exon–intron structures of *VvNRT1* genes were examined using MEME and GSDS 2.0, respectively. A maximum-likelihood phylogenetic tree was generated to assess the

relationships among evolutionary clades, motif composition, and gene structural features (Fig. 2a), which was consistent with the clustering pattern observed in Fig. 1a. The identification of conserved motifs provides crucial evidence for understanding evolutionary relationships. In total, 10 conserved motifs were identified, with motif lengths ranging from 17 to 41 amino acids (Figs. 2b and S2). In groups and , *VvNRT1.62*, *VvNRT1.43*, *VvNRT1.15*, *VvNRT1.30*, and *VvNRT1.53* each contained only two motifs, whereas *VvNRT1.40*, *VvNRT1.55*, *VvNRT1.33*, and *VvNRT1.44* in groups I, , and possessed a single motif. Members within the same clade exhibited similar motif positions and distribution patterns, which were largely conserved across groups I–. Conversely, group V contained markedly fewer motifs than the other groups.

The exon–intron architecture is a key component of the gene structural architecture. Accordingly, the structural features of all 65 *VvNRT1* genes were analyzed, including the number, length, and position of exons and introns (Fig. 2c). Genes belonging to the same phylogenetic subfamily displayed highly conserved gene structures, further supporting the established classification of grapevine *NRT1s*. In groups I, , and , *VvNRT1.62*, *VvNRT1.40*, *VvNRT1.8*, *VvNRT1.15*, and *VvNRT1.30* each consisted of a single exon. Most group I genes contained five or more exons, with *VvNRT1.63* and *VvNRT1.64* each containing nine exons. Genes in group generally possessed four to six exons, whereas those in subgroups and typically contained four exons. In contrast, group V genes exhibited a wider range of exon numbers, from three to six, and their gene lengths were notably shorter than those of other groups. All members of group had contained both 3'-UTR and 5'-UTR regions, whereas group V genes lacked one or both UTRs. These variations in gene structure may underlie the functional divergence observed among VvNRT1 family members.

Cis-regulatory element analysis of VvNRT1s

The regulatory element composition of *VvNRT1* genes was analyzed, and the genes were classified into distinct clusters according to their response patterns to different regulatory signals. Each cluster exhibited characteristic regulatory profiles associated with specific environmental and developmental cues (Fig. 3a).

In cluster , most *VvNRT1* genes exhibited strong responsiveness to stress-related elements, including defense and anaerobic induction elements (green, red, and purple squares), indicating their potential involvement in stress responses. Cluster was mainly characterized by *VvNRT1* genes responsive to hormone-related regulatory elements, such as auxin and salicylic acid (orange, brown, and light pink squares). Cluster displayed broad associations with developmental regulation, particularly seed-specific regulation and meristem-related elements (blue squares), suggesting an important role in plant growth regulation. The genes in cluster exhibited the most diverse response patterns, with the largest proportion being responsive to methyl jasmonate (MeJA; 36 genes), highlighting a prominent role in stress and hormone signaling crosstalk. In contrast, cluster V presented a relatively limited responsiveness, while some genes were associated with low-temperature and circadian control

elements (light blue squares), and overall contained fewer *VvNRT1* genes, especially those related to seed-specific regulation and gibberellin responses.

Consistent with these observations, heatmap analysis (Fig. 3b) revealed distinct regulatory distributions of *VvNRT1* genes across the examined biological processes. In cluster Ⅰ, a substantial number of *VvNRT1* genes (46) were responsive to MeJA, whereas cluster Ⅱ exhibited strong responsiveness to auxin-related elements (41 genes). In contrast, cluster Ⅲ contained fewer *VvNRT1* genes responsive to low-temperature and anaerobic induction signals.

Overall, these results indicate that *VvNRT1* genes are differentially regulated by environmental stress, hormone-related signals, and developmental cues. The clustering patterns based on cis-regulatory elements further underscored the functional complexity of *VvNRT1* genes in grapevine growth regulation and stress response.

Tissue-specific expression profile of VvNRT1s

To further clarify the potential roles of *VvNRT1s*, expression profiles across 19 different organs or tissues at multiple developmental stages were obtained from the BAR database (Fig. 4). The *VvNRT1* genes exhibited widespread expression across nearly all examined tissues. Evident expression differences were observed among phylogenetic groups, where members of Groups I and II demonstrated broader expression ranges across diverse tissues than those belonging to other groups. Several genes showed significantly elevated expression levels in specific tissues or developmental stages. For example, *VvNRT1.7* and *VvNRT1.21* showed the significantly higher expression in roots than other tissues or organs, whereas *VvNRT1.34* and *VvNRT1.38* reached peak expression during the flowering stage. Moreover, *VvNRT1.1* and *VvNRT1.60* exhibited the highest expression levels at the bud swell and mature fruit stages, respectively. In addition, some genes, such as *VvNRT1.34*, were highly expressed in multiple tissues, whereas others, including *VvNRT1.9* and *VvNRT1.10*, consistently maintained low expression levels in most tissues. Furthermore, all genes in group Ⅲ demonstrated uniformly lower expression across all examined tissues and organs than those in other subgroups. Based on these expression patterns, *VvNRT1* genes may exhibit functional differentiation that supports coordinated nitrogen uptake and transport across grapevine tissues. Collectively, these genes represent potential targets for improving nitrogen use efficiency and may serve as integral regulators of grapevine growth and responses to environmental stress.

Expression profiles of VvNRT1s after KNO_3 treatment and salt stress

Based on the above analyses, numerous hormone- and stress-related cis-acting elements were identified in the promoters of *VvNRT*1 genes. In addition, previous studies have shown that *NPF5.15* and *NPF7.3* play important roles in salt tolerance in *Arabidopsis* [23]. To examine the responses of *VvNRT1* genes to NO_3^- treatment and salt stress, their expression levels were analyzed in grape leaves and roots at 10 min, 0.5 h, 2 h, and 8 h after NO_3^- treatment, and at 6, 12, 24, and 48 h after salt treatment. The experiment was conducted using own-rooted seedlings of the '*Shine Muscat*' cultivar, which was

selected for its wide cultivation, economic value, and strong stress tolerance, thereby enabling the assessment of expression patterns of selected *VvNRT1s* under stress conditions. Four grape genes homologous to *Arabidopsis AtNPF4.3*, *AtNPF5.10*, *AtNPF5.15*, and *AtNPF7.3* were examined, corresponding to *VvNRT1.35*, *VvNRT1.59*, *VvNRT1.19*, and *VvNRT1.47*, respectively.

The expression levels of *VvNRT1.19* and *VvNRT1.47* were higher than those of the 0 h control under both NO_3^- treatment and salt stress. Under NO_3^- treatment, a progressive increase in expression was observed in the roots over time, with the expression in both roots and leaves reaching a maximum at 8 h (Fig. 5a). Under salt stress, the expression in both roots and leaves peaked at 6 h, after which the expression of *VvNRT1.19* in the roots gradually declined (Fig. 5b). Although *VvNRT1.35* and *VvNRT1.59* demonstrated increased expression in roots under salt stress compared with the 0 h control, their expression in leaves under both nitrate and salt treatments displayed time points at which transcript levels were reduced relative to the control (Fig. 5).

VvNRT1.19 and VvNRT1.47 overexpression enhanced nitrogen use efficiency and salt tolerance in Arabidopsis

Both *VvNRT1.19* and *VvNRT1.47* were transcriptionally induced in grape roots and leaves at 10 min, 0.5 h, 2 h, and 8 h following NO_3^- treatment, as well as at 6, 12, 24, and 48 h after salt treatment. *VvNRT1.19* and *VvNRT1.47* were highly homologous to *AtNPF5.15* and *AtNPF7.3*, respectively, which are key members of the NO_3^- transporter family known to contribute to nitrogen use efficiency, although their roles in plant salt tolerance remain unclear. To examine the functions of *VvNRT1.19* and *VvNRT1.47* in responses to NO_3^- availability and salt stress, 12 *VvNRT1.19*-overexpressing (*VvNRT1.19-OE*) lines and 10 *VvNRT1.47*-overexpressing (*VvNRT1.47-OE*) *Arabidopsis* lines were generated via *Agrobacterium*-mediated transformation. qPCR analysis confirmed the markedly elevated transcript levels of both genes in the leaves of the transgenic lines (Fig. 6a and b). Based on these results, the lines showing the highest expression levels of *VvNRT1.19* (#11) and *VvNRT1.47* (#10) were selected for further analyses. To determine whether the overexpression of *VvNRT1.19* and *VvNRT1.47* influenced nitrogen use efficiency and salt tolerance, transgenic and wild-type (WT) plants were grown under 0, 1, and 5 mM KNO_3 conditions and subjected to 200 mM NaCl stress.

Under all tested KNO_3 concentrations, the WT seedlings displayed inhibited root development, cotyledon yellowing, and retarded growth, whereas the overexpression lines maintained well-developed root systems (Fig. 6c) and vigorous seedling growth (Fig. 6d). At 1 and 5 mM KNO_3, the average root length of the overexpression lines was significantly greater than that of WT plants (Fig. 6f). Under 0 and 1 mM KNO_3 conditions, both the number of lateral roots and cotyledon area were also significantly increased in the overexpression lines compared with WT plants (Fig. 6g and h). These results indicated that the overexpression of *VvNRT1.47* and *VvNRT1.19* enhanced NO_3^- uptake and utilization, thereby promoting plant growth under both nitrate-deficient and nitrate-sufficient conditions. In addition, the performance of overexpression lines was assessed under salt stress (200 mM NaCl). The WT seedlings exhibited severe

growth inhibition and pronounced leaf yellowing, whereas *VvNRT1.47-OE* and *VvNRT1.19-OE* seedlings maintained comparatively better growth and more normal morphology (Fig. 6e). Moreover, the survival rates of the overexpression lines were significantly higher than those of WT plants at both day 8 and day 14 (Fig. 6i), suggesting that *VvNRT1.47* and *VvNRT1.19* contributed to improved survival under salt stress conditions.

Discussion

NRT1 proteins represent the largest and most functionally diverse NO_3^- transporter group in plants and are central to plant growth regulation, stress responses, and NO_3^- uptake and metabolism. Genome-wide analyses of *NRT1* gene families have been reported in several species, including *Sorghum bicolor* [28], *Eucalyptus grandis* [29], *Setaria italica* [30], *Brassica rapa* [31], and *Cocos nucifera L.* [32]. However, a systematic genome-wide investigation of the NRT1 family in grapevine (*Vitis vinifera*) has not been performed. Here, 65 *VvNRT1* genes were identified in grapevine and further characterized by phylogenetic classification, gene structure analysis, and expression profiling. These results provide evidence for the evolutionary features of grapevine NRT1s and support their potential involvement in nitrogen utilization and stress adaptation.

The 65 *VvNRT1* genes identified in this study exceeded the 53 NRT1 members reported in *Arabidopsis* [33], indicating an expanded *NRT1* repertoire in grapevine. Phylogenetic analysis divided *VvNRT1s* into five groups (Ⅰ–Ⅴ), differing from the eight-group classification commonly reported in *Arabidopsis* and rice [33], which may reflect the grapevine-specific evolutionary history, including polyploidization and lineage-specific duplication. Chromosomal mapping revealed an enrichment of *VvNRT1s* on chromosome 18 (Fig. 1b), where multiple tandemly duplicated genes (e.g., *VvNRT1.59–VvNRT1.65*) were concentrated, suggesting that tandem duplication contributed substantially to this clustering. Such clustering may facilitate the coordinated regulation of genes related to N transport or stress responses in grapevine.

The duplication analysis indicated that 64.62% of *VvNRT1s* were associated with segmental duplication, whereas 30.77% formed tandem duplication pairs (Fig. 1b), indicating that both duplication modes contributed to family expansion, similar to the pattern reported for the apple *NRT1* family [34]. Tandem duplicates often retain similar functions, whereas segmental duplicates more frequently diverge functionally [35]. Consistent with this tendency, tandemly duplicated genes, such as *VvNRT1.49–VvNRT1.51*, displayed similar motif compositions and tissue expression patterns, whereas the segmentally duplicated pair *VvNRT1.1* and *VvNRT1.6* differed markedly in cis-regulatory element profiles (Fig. 3), implying possible divergence associated with environmental adaptation.

Conserved motif and gene structure analyses further indicated that genes within the same phylogenetic group generally shared similar motif compositions and exon–intron architectures (Fig. 2), supporting the reliability of the classification. For instance, Group Ⅱ members *VvNRT1.63* and *VvNRT1.64* both contained nine exons and motifs 1–10, whereas Group Ⅲ members carried fewer motifs, potentially reflecting their functional specialization. Notably, *VvNRT1.40* and *VvNRT1.55* contained a single exon and one motif.

Comparable compact *NRT1* genes have also been reported in *Arabidopsis* (e.g., *AtNPF2.9*) and proposed to enable rapid responses to environmental signals via a simplified regulatory architecture [36].

Cis-element analysis suggested that *VvNRT1* promoters were enriched in elements related to hormone responses (e.g., MeJA and ABA), stress responses (e.g., low temperature and anoxia), and growth and developmental regulation (Fig. 3), which can support a role in multi-signal integration during grapevine growth and stress adaptation. Notably, Group Ⅱ contained abundant stress-responsive elements and was enriched in hormone-related elements, suggesting a contribution to hormone–stress crosstalk, consistent with reports that rice NPFs participate in the coordinated regulation of salt stress responses and ABA signaling [37–38].

Tissue-specific expression profiling revealed distinct expression patterns among *VvNRT1s*. *VvNRT1.7* and *VvNRT1.21* were predominantly expressed in roots, suggesting roles in nitrate uptake, whereas *VvNRT1.34* and *VvNRT1.38* showed elevated expression during flowering, indicating their potential involvement in the nitrogen supply to reproductive organs. In addition, *VvNRT1.1* exhibited high expression during bud swelling, implying a role in bud development (Fig. 4). This expression specificity resembled the tissue-based functional differentiation reported for *Arabidopsis NRT1s*, such as *AtNPF6.3*, which functions in root NO_3^- uptake, and *AtNPF7.2*, which mediates NO_3^- redistribution in leaves [39–40]. These observations suggest that the grapevine *NRT1* family retained conserved functional patterns while acquiring specialized expression profiles in newly expanded members to accommodate the perennial growth habit of fruit trees.

The functions of *NRT* genes in *Arabidopsis thaliana* have been extensively characterized, with different subfamilies participating in N uptake, transport, signaling, and stress adaptation. *AtNRT* genes primarily act as molecular carriers that mediate NO_3^- uptake and internal allocation. The two major subfamilies operate under distinct nitrogen regimes. The NRT1 (NPF) subfamily mainly mediates low-affinity transport under high nitrogen conditions (soil NO_3^- > 1 mmol/L), facilitating NO_3^- uptake or its translocation within the plant (root → stem → leaf; source organ → sink organ) [41]. For instance, *AtNRT1.5* [40] mediates root-to-shoot NO_3^- translocation, whereas *AtNRT1.4* [42] is involved in NO_3^- storage in leaves. Notably, certain members, such as *AtNRT1.1* [43], act as “dual-affinity transporters”, enabling NO_3^- absorption across a broad range of external concentrations. In contrast, the NRT2 subfamily specializes in high-affinity nitrate transport under low nitrogen availability (soil NO_3^- < 0.5 mmol/L) and plays a critical role in nitrogen deficiency adaptation [41]. Representative genes, such as *AtNRT2.1* and *AtNRT2.2*, are predominantly expressed in root epidermal cells and root hairs, where they directly absorb NO_3^- from the soil [44].

In this study, *VvNRT1.19* and *VvNRT1.47*, which showed the highest homology to *Arabidopsis AtNPF5.15* and *AtNPF7.3*, respectively, were significantly upregulated under high-N conditions (Fig. 5a). Both genes were strongly induced by salt stress (Fig. 5b), indicating that they responded to N signaling and participated in salt stress responses.

Subsequently, *VvNRT1.19* and *VvNRT1.47* were cloned to generate 12 *VvNRT1.19-OE* and 10 *VvNRT1.47-OE Arabidopsis* lines. Lines exhibiting the highest expression levels were selected for the validation of nitrogen use efficiency and salt tolerance (Fig. 6a and b). Overexpression of *VvNRT1.19* or *VvNRT1.47* resulted in improved nitrogen use efficiency and enhanced salt tolerance under nitrate treatment (Fig. 6c–i), demonstrating that both genes contributed to the coordinated regulation of nitrogen utilization and salt tolerance.

In summary, this study presents a comprehensive analysis of the *NRT1* gene family in grapevine. By integrating bioinformatics and experimental approaches, this study defined the key structural, evolutionary, and functional features of *VvNRT1s* and established a framework for further investigation. This study provides the first evidence that *VvNRT1.19* and *VvNRT1.47* function as N-responsive genes involved in both N metabolism and salt stress responses, offering insights for future functional studies of *NRT1* genes in grapevine and other plant species.

Conclusion

In this study, 65 intact NRT1 genes were systematically identified in the grapevine genome and classified into five distinct phylogenetic groups. Duplication pattern analyses indicated that both segmental and tandem duplication events contributed to the expansion of the *VvNRT1* gene family. Combined analyses of promoter cis-elements and tissue-specific expression patterns suggested that *VvNRT1* genes participated in grapevine growth, environmental stress responses, and nitrogen regulation.

Moreover, several *VvNRT1* members exhibited pronounced transcriptional induction in roots and leaves in response to NO_3^- and salt treatments. Functional assays using transgenic Arabidopsis plants further demonstrated that ectopic expression of *VvNRT1.19* and *VvNRT1.47* significantly enhanced nitrogen use efficiency and salt tolerance.

In summary, these results extend the current understanding of the functional diversity of the *VvNRT1* family and highlight its potential value in improving nutrient acquisition and stress adaptability in plants.

Materials and methods

Identification of VvNRT1 Genes

Arabidopsis NRT1 protein sequences were obtained from the TAIR[1] database and used as queries to screen the grapevine genomes. BLASTP [45] searches were performed against the Phytozome2[2] and Winberige[3] databases to identify putative *VvNRT1* members, and only candidates with E-values below 1×10^{-10} were retained.

To confirm domain composition, conserved LRR and extensin domains were examined using the NCBI Conserved Domain Database and SMART. Basic physicochemical properties, including protein length,

molecular weight, and theoretical isoelectric point, were predicted using the ExPASy ProtParam server[4].

Phylogenetic and Collinearity Analysis

Full-length NRT1 protein sequences from grapevine and Arabidopsis were aligned using ClustalW. A maximum-likelihood phylogenetic tree was constructed using MEGA 7.0, and branch support was assessed using 1000 bootstrap replicates [46]. Collinearity and gene duplication events were analyzed using MCScanX [47]. Chromosomal location data were obtained from the Winberge database, and syntenic relationships were visualized using TBtools [48].

Gene Structure and Motif Analysis

The exon–intron organization of *VvNRT1* genes was analyzed using the Gene Structure Display Server[5] [49]. Gene structure diagrams were generated using TBtools. Conserved protein motifs were identified using MEME[6] [50], and motif distribution patterns among VvNRT1 proteins were examined to evaluate their structural conservation.

Promoter Analysis

Upstream sequences (2 kb) of each VvNRT1 gene were extracted using TBtools. Cis-regulatory elements were predicted with PlantCARE[7], and their distribution patterns were visualized.

Tissue Expression Analysis

Transcriptome datasets were retrieved from the BAR database[8], covering roots, stems, leaves, buds, flowers, fruits, seedlings, and pollen. After removing low-abundance transcripts, expression values were $\log_2$-transformed and normalized. Heatmaps were generated using TBtools.

Plant Materials and Treatments

One-year-old own-rooted grapevine seedlings (*Vitis vinifera* L. cv. Shine Muscat) were obtained from Shandong Zhichang Agricultural Science and Technology Development Co., Ltd. Uniform seedlings were selected and grown under greenhouse conditions (12 h light/12 h dark; 25–28°C day/5–10°C night; 55–65% relative humidity). Seedlings were cultivated in plastic pots containing washed sand and treated with 15 mM KNO_3 or 200 mM NaCl to evaluate nitrate and salt responses. Leaves and roots were collected at designated time points, immediately frozen in liquid nitrogen, and stored at − 80°C.

qRT-PCR

Gene-specific primers were designed using SnapGene. Total RNA was extracted using the QuickRNA kit, followed by genomic DNA removal. RNA quality was assessed using NanoDrop and Bioanalyzer

platforms. cDNA synthesis was performed using PrimeScript RT Master Mix. qRT-PCR was conducted on a CFX96 system using TB Green chemistry, with *VvUBI* serving as the internal reference gene [44]. Each reaction contained 2 μL of cDNA. Amplification was performed for 40 cycles following initial denaturation, and melting curve analysis was used to verify primer specificity. Relative gene expression levels were calculated using the $2^{-}\Delta\Delta Ct$ method [51].

Vector Construction and Plant Transformation

Full-length coding sequences (CDS) of *VvNRT1.47* (1815 bp) and *VvNRT1.19* (324 bp) were amplified from cDNA synthesized from leaves of own-rooted 'Shine Muscat' grapevine seedlings and verified by sequencing. Validated CDS fragments were cloned into the plant expression vector pBWA(V)BS under the control of the CaMV 35S promoter using the MultiF Seamless Assembly system (ABclonal). Recombinant plasmids pBWA(V)BS-VvNRT1.47 and pBWA(V)BS-VvNRT1.19 were introduced into *Agrobacterium tumefaciens* strain GV3101. Primer sequences used for gene amplification are listed in Table S1. Transgenic *Arabidopsis thaliana* plants harboring *35S::VvNRT1.47* and *35S::VvNRT1.19* constructs were generated via *Agrobacterium*-mediated transformation.

Declarations

Ethics approval and consent to participate

Not applicable.

Consent for publication

Not applicable.

Competing interests

The authors declare that they have no competing interests.

Author details

[1] College of Horticulture and Landscape Architecture, Yangzhou University, Yangzhou 225009, China

[2] Shandong Academy of Grape, Shandong Academy of Agricultural Sciences, Jinan 250100, China

[3] Weifang University, Weifang 261061, China

Funding

This study was supported by the Natural Science Foundation of Shandong Province (Grant No. ZR2023MC101) and Agricultural Science and Technology Innovation Project of Shandong Academy of

Agricultural Sciences(Grant No. CXGC2026A47), and Science and Technology Support Plan for Youth Innovation of Colleges and Universities of Shandong Province of China (2024KJI023) and Jinan Comprehensive Experiment Station of National Grape Industry Technology System (CARS-29-16).

Author Contribution

Chen Zhou : Conceptualization, Sample preparation and analysis, Methodology, Data curation, Writing-original draft, Supervision. Yingchun Chen : Data curation, Methodology, Formal analysis. Kai Liu : Methodology, Conceptualization, Supervision. Xiujie Li : Conceptualization, Supervision. Xuehui Zhao : Data curation, Conceptualization. Bo Li : Conceptualization, Supervision. Li Liu : Conceptualization, Writing – review & editing, Supervision. Zhaosen Xie : Conceptualization, Methodology, Supervision.

Data Availability

All data generated or analyzed during this study are included in this published article. The genome-wide sequence data of *Vitis vinifera* L. supporting the findings of this study are publicly available in the NCBI database ([https://www.ncbi.nlm.nih.gov/](https:/www.ncbi.nlm.nih.gov)) and Winberige database (http://www.winberige.cc/index.php).

References

1. Wang Q, Li S, Li J, Huang D. The Utilization and Roles of Nitrogen in Plants. Forests 2024, 15(7).
2. Hachiya T, Sakakibara H. Interactions between nitrate and ammonium in their uptake, allocation, assimilation, and signaling in plants. J Exp Bot 2016.
3. Nedelyaeva OI, Khramov DE, Balnokin YV, Volkov VS. Functional and Molecular Characterization of Plant Nitrate Transporters Belonging to NPF (NRT1/PTR) 6 Subfamily. Int J Mol Sci 2024, 25(24).
4. TONG Y-p CAIC, LIU, Q-y. LI J-y, LI Z-s: Recent advances in molecular biology of nitrate transporters in higher plants. J Plant Nutr Fertilizers. 2004;10(4):433–40.
5. Orsel M, Filleur S, Fraisier V, Daniel-Vedele F. Nitrate transport in plants: which gene and which control? J Exp Bot. 2002;53(370):825–33.
6. Wen Z, Kaiser BN. Unraveling the functional role of NPF6 transporters. Front Plant Sci. 2018;9:973.
7. Rahmat Z, Sohail MN, Perrine-Walker F, Kaiser BN. Balancing nitrate acquisition strategies in symbiotic legumes. Planta. 2023;258(1):12.
8. Kanno Y, Kamiya Y, Seo M. Nitrate does not compete with abscisic acid as a substrate of AtNPF4. 6/NRT1. 2/AIT1 in Arabidopsis. Plant Signal Behav. 2013;8(12):e26624.
9. Léran S, Garg B, Boursiac Y, Corratgé-Faillie C, Brachet C, Tillard P, Gojon A, Lacombe B. AtNPF5. 5, a nitrate transporter affecting nitrogen accumulation in Arabidopsis embryo. Sci Rep. 2015;5(1):7962.

10. Siangliw JL, Ruangsiri M, Theerawitaya C, Cha-Um S, Poncheewin W, Songtoasesakul D, Thunnom B, Ruanjaichon V, Toojinda T. Contrasting Alleles of OsNRT1. 1b Fostering Potential in Improving Nitrogen Use Efficiency in Rice. Plants. 2024;13(20):2932.
11. Duan D, Zhang H. A single SNP in NRT1. 1B has a major impact on nitrogen use efficiency in rice. Sci China Life Sci. 2015;58(8):827.
12. Cao H, Liu Z, Guo J, Jia Z, Shi Y, Kang K, Peng W, Wang Z, Chen L, Neuhaeuser B. ZmNRT1. 1B (ZmNPF6. 6) determines nitrogen use efficiency via regulation of nitrate transport and signalling in maize. Plant Biotechnol J. 2024;22(2):316–29.
13. Wang Q, Liu C, Dong Q, Huang D, Li C, Li P, Ma F. Genome-wide identification and analysis of apple NITRATE TRANSPORTER 1/PEPTIDE TRANSPORTER family (NPF) genes reveals MdNPF6. 5 confers high capacity for nitrogen uptake under low-nitrogen conditions. Int J Mol Sci. 2018;19(9):2761.
14. Zhang H, Zhao X, Sun Q, Yan C, Wang J, Yuan C, Li C, Shan S, Liu F. Comparative transcriptome analysis reveals molecular defensive mechanism of Arachis hypogaea in response to salt stress. Int J Genomics 2020, 2020(1):6524093.
15. Yang D-c, Xu Q, Zhao F-g, Liu M, Liu X. Effects of NaCl stress on nitrogen metabolism and related gene expression of rice with different resistance. 2020.
16. Liu R, Cui B, Jia T, Song J. Role of Suaeda salsa SsNRT2. 1 in nitrate uptake under low nitrate and high saline conditions. Plant Physiol Biochem. 2021;159:171–8.
17. Liu R, Cui B, Lu X, Song J. The positive effect of salinity on nitrate uptake in Suaeda salsa. Plant Physiol Biochem. 2021;166:958–63.
18. Sena F, Kunze R. The K+ transporter NPF7. 3/NRT1. 5 and the proton pump AHA2 contribute to K+ transport in Arabidopsis thaliana under K + and NO3-deficiency. Front Plant Sci. 2023;14:1287843.
19. Wang X, Liu Y, Li W, Ma X, Wang W, Jiang Z, Wang Y, Li L, Hu B, Chu C. OsNRT1. 1B-OsCNGC14/16-Ca2+-OsNLP3 Pathway: Phosphorylation-Mediated Maintenance of Nitrogen Homeostasis. Adv Sci. 2025;12(43):e07919.
20. Sa G, Yao J, Deng C, Liu J, Zhang Y, Zhu Z, Zhang Y, Ma X, Zhao R, Lin S. Amelioration of nitrate uptake under salt stress by ectomycorrhiza with and without a Hartig net. New Phytol. 2019;222(4):1951–64.
21. Keller M, Koblet W. Dry matter and leaf area partitioning, bud fertility and second season growth of Vitis vinifera L.: Responses to nitrogen supply and limiting irradiance. Vitis. 1995;34(2):77–83.
22. Stefanello LO, Schwalbert R, Marques AR, Tarouco CP, Vitto BB, Krug A, dos Santos JJ, Galarza BP, Zalamena J, dos Santos HP. Photosynthetic activity and grape yield of'Alicante Bouschet'(Vitis vinifera L.) grapevines submitted to nitrogen supply methods and doses. Vitis. 2020;59:133–40.
23. Zhang C, Lu X, Yan H, Gong M, Wang W, Chen B, Ma S, Li S. Nitrogen application improves salt tolerance of grape seedlings via regulating hormone metabolism. Physiol Plant. 2023;175(2):e13896.
24. Altemose N, Logsdon GA, Bzikadze AV, Sidhwani P, Langley SA, Caldas GV, Hoyt SJ, Uralsky L, Ryabov FD, Shew CJ. Complete genomic and epigenetic maps of human centromeres. Science.

2022;376(6588):eabl4178.

25. Yang Z, Mei J, Zheng W, Khan FS, Bhuiyan MN, Wang K, Rhaman MS, Abe-Kanoh N, Ji W. Identification of Grape NRT Gene Family and Analysis of Its Expression in Leaves Under Nitrogen-Deficiency Stress. Horticulturae. 2025;11(3):252.
26. Monte R, Tomasi N, Cesco S, Zamboni A, Varanini Z, Pinton R. Physiological and molecular characterization of nitrate uptake mechanisms in roots of grapevine (Vitis vinifera L.) cultivars. 2009.
27. Shi X, Cao S, Wang X, Huang S, Wang Y, Liu Z, Liu W, Leng X, Peng Y, Wang N. The complete reference genome for grapevine (Vitis vinifera L.) genetics and breeding. Hortic Res. 2023;10(5):uhad061.
28. Zhiqiang G, Yuexiu L, Fan F, Lixun Z, Jiali F, Xiaodong J, Jinhui L, Chunlai Z. Genome-wide Identification of NRT1 Gene, Expression Profiling and DNA Variation Analysis in Sorghum. J Laser Biology/Acta Laser Biology Sinica 2021, 30(5).
29. Li G, Yang D, Hu Y, Xu J, Lu Z. Genome-wide identification and expression analysis of nitrate transporter (NRT) gene family in Eucalyptus grandis. Genes. 2024;15(7):930.
30. Cheng J, Tan H, Shan M, Duan M, Ye L, Yang Y, He L, Shen H, Yang Z, Wang X. Genome-wide identification and characterization of the NPF genes provide new insight into low nitrogen tolerance in Setaria. Front Plant Sci. 2022;13:1043832.
31. Zhang Y, Ritonga FN, Zhang S, Wang F, Li J, Gao J. Genome-Wide Identification of the NRT1 Family Members and Their Expression under Low-Nitrate Conditions in Chinese Cabbage (Brassica rapa L. ssp. pekinensis). Plants. 2023;12(22):3882.
32. Liu X, Li J, Luo D, Ding H, Zhang M, Gao P, Mehvish A, Sun X, Tong C, Wu Q. Genome-wide characterization of the NRT1 family members under cold stress in Coconut (Cocos nucifera L). Sci Hort. 2025;341:113959.
33. Léran S, Varala K, Boyer J-C, Chiurazzi M, Crawford N, Daniel-Vedele F, David L, Dickstein R, Fernandez E, Forde B. A unified nomenclature of NITRATE TRANSPORTER 1/PEPTIDE TRANSPORTER family members in plants. Trends Plant Sci. 2014;19(1):5–9.
34. Tahir MM, Wang H, Ahmad B, Liu Y, Fan S, Li K, Lei C, Shah K, Li S, Zhang D. Identification and characterization of NRT gene family reveals their critical response to nitrate regulation during adventitious root formation and development in apple rootstock. Sci Hort. 2021;275:109642.
35. Laha SD, Dutta S, Schäffner AR, Das M. Gene duplication and stress genomics in Brassicas: Current understanding and future prospects. J Plant Physiol. 2020;255:153293.
36. Wang Y-Y, Tsay Y-F. Arabidopsis nitrate transporter NRT1. 9 is important in phloem nitrate transport. Plant Cell. 2011;23(5):1945–57.
37. Hang J, Wu B, Qiu D, Yang G, Fang Z, Zhang M. OsNPF3. 1, a nitrate, abscisic acid and gibberellin transporter gene, is essential for rice tillering and nitrogen utilization efficiency. J Integr Agric. 2024;23(4):1087–104.

38. Islam MS. Sensing and uptake of nitrogen in rice plant: a molecular view. Rice Sci. 2019;26(6):343–55.
39. LIU H, LIU Q, GAO X, FU X. Role of nitrogen sensing and its integrative signaling pathways in shaping root system architecture. Eng Agric. 2022;9(3):316–32.
40. Li J-Y, Fu Y-L, Pike SM, Bao J, Tian W, Zhang Y, Chen C-Z, Zhang Y, Li H-M, Huang J. The Arabidopsis nitrate transporter NRT1. 8 functions in nitrate removal from the xylem sap and mediates cadmium tolerance. Plant Cell. 2010;22(5):1633–46.
41. Chiba Y, Shimizu T, Miyakawa S, Kanno Y, Koshiba T, Kamiya Y, Seo M. Identification of Arabidopsis thaliana NRT1/PTR FAMILY (NPF) proteins capable of transporting plant hormones. J Plant Res. 2015;128(4):679–86.
42. Krapp A, David LC, Chardin C, Girin T, Marmagne A, Leprince A-S, Chaillou S, Ferrario-Méry S, Meyer C, Daniel-Vedele F. Nitrate transport and signalling in Arabidopsis. J Exp Bot. 2014;65(3):789–98.
43. Bouguyon É, Brun F, Meynard D, Kubeš M, Pervent M, Léran S, Lacombe B, Krouk G, Guiderdoni E, Zažímalová E. Multiple mechanisms of nitrate sensing by Arabidopsis nitrate transceptor NRT1. 1. Nat plants. 2015;1(3):1–8.
44. Ho C-H, Lin S-H, Hu H-C, Tsay Y-F. CHL1 functions as a nitrate sensor in plants. Cell. 2009;138(6):1184–94.
45. Altschul SF, Gish W, Miller W, Myers EW, Lipman DJ. Basic local alignment search tool. J Mol Biol. 1990;215(3):403–10.
46. Thompson JD, Gibson TJ, Higgins DG. Multiple sequence alignment using ClustalW and ClustalX. Curr protocols Bioinf 2003(1):2.3. 1-2.3. 22.
47. Wang Y, Tang H, DeBarry JD, Tan X, Li J, Wang X, Lee T-h, Jin H, Marler B, Guo H. MCScanX: a toolkit for detection and evolutionary analysis of gene synteny and collinearity. Nucleic Acids Res. 2012;40(7):e49–49.
48. Chen C, Chen H, Zhang Y, Thomas HR, Frank MH, He Y, Xia R. TBtools: an integrative toolkit developed for interactive analyses of big biological data. Mol Plant. 2020;13(8):1194–202.
49. Guo A-Y, Zhu Q-H, Chen X, Luo J-C. GSDS: a gene structure display server. Yi chuan= Hereditas. 2007;29(8):1023–6.
50. Bailey TL, Boden M, Buske FA, Frith M, Grant CE, Clementi L, Ren J, Li WW, Noble WS. MEME SUITE: tools for motif discovery and searching. Nucleic Acids Res. 2009;37(suppl2):W202–8.
51. Liu K, Yang A, Yan J, Liang Z, Yuan G, Cong P, Zhang L, Han X, Zhang C. MdAIL5 overexpression promotes apple adventitious shoot regeneration by regulating hormone signaling and activating the expression of shoot development-related genes. Hortic Res. 2023;10(11):uhad198.

Footnotes

1. https://www.arabidopsis.org/browse/gene_family
2. https://phytozome-next.jgi.doe.gov/blast-search

3. http://www.winberige.cc/ftp.html
4. https://web.expasy.org/protparam/
5. http://gsds.cbi.pku.edu.cn/
6. https://meme-suite.org/meme/tools/meme
7. http://bioinformatics.psb.ugent.be/webtools/plantcare/html/
8. https://bar.utoronto.ca/efp_grape/cgi-bin/efpWeb.cgi

Figures

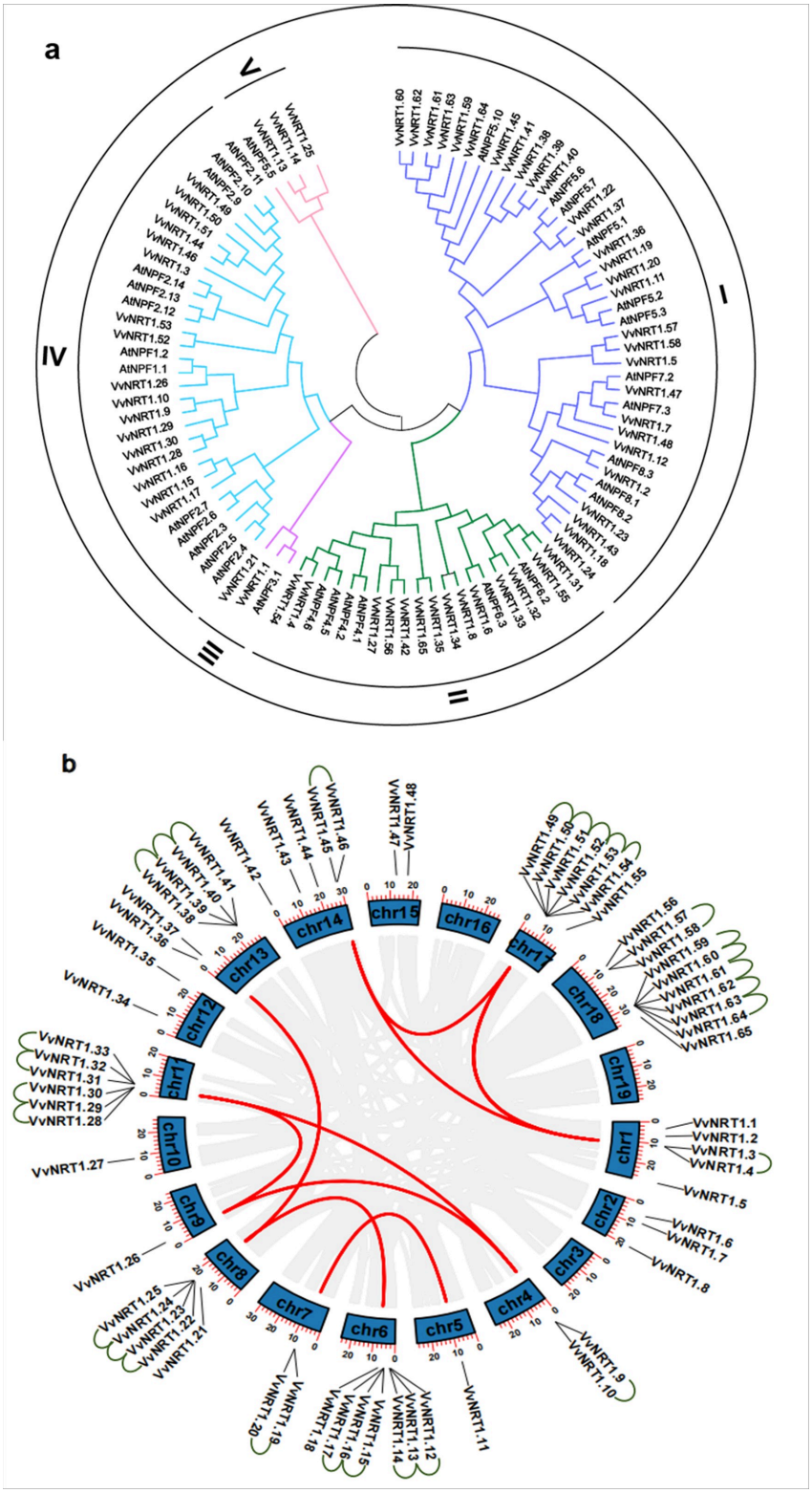


Figure 1

Phylogenetic and synteny analyses of the NRT1 gene family. **a** Phylogenetic relationship between NRT1 proteins from grapevine and *Arabidopsis*. **b** Duplication events and chromosomal distribution of *VvNRT1s*. Segmentally duplicated gene pairs are linked by red lines, and tandemly duplicated genes are linked by green lines.

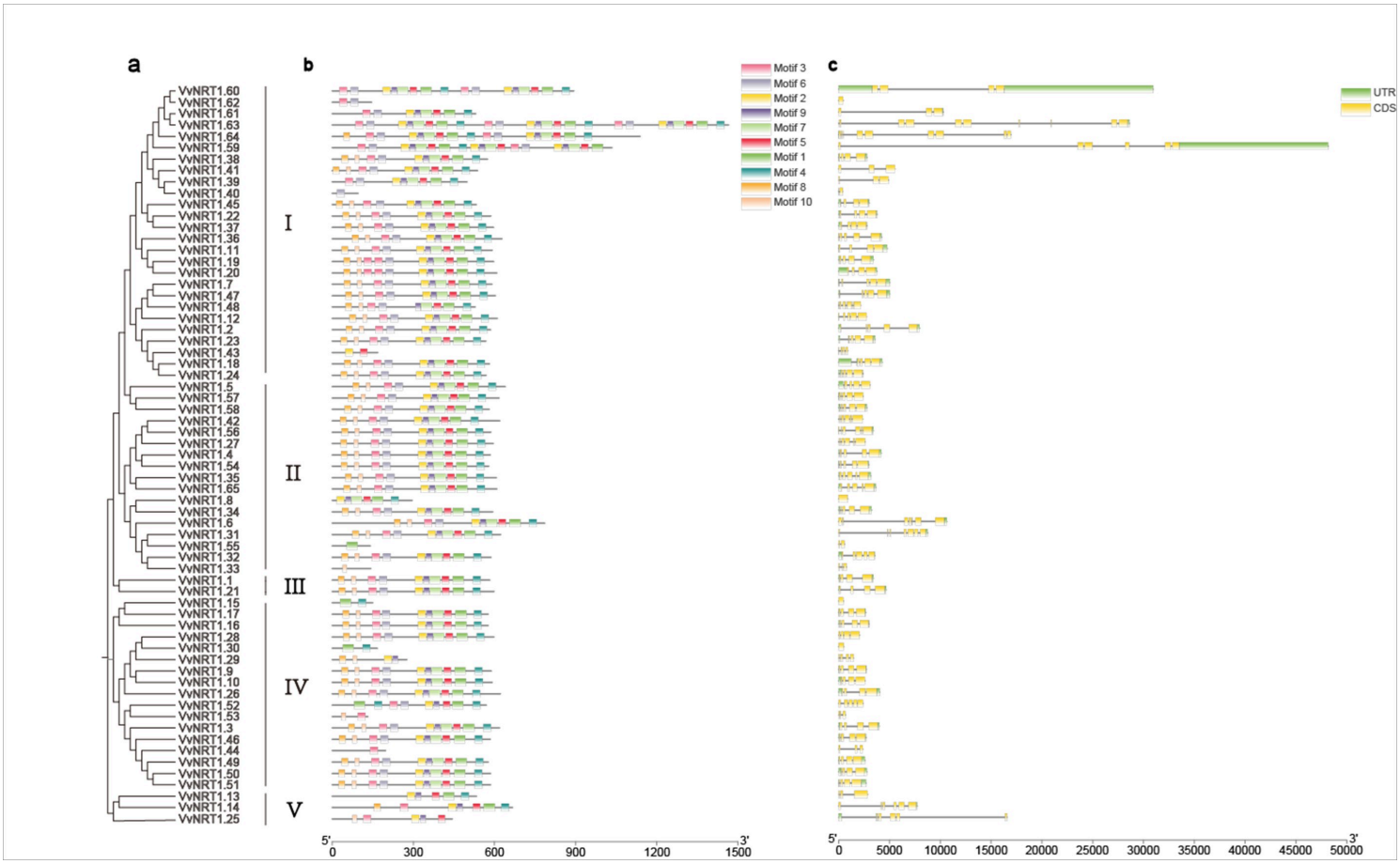


Figure 2

Conserved motifs and structures of *VvNRT1* genes. **a** Phylogenetic tree of VvNRT1s. **b** Conserved motifs within *VvNRT1s*, represented by colored squares for motifs 1–10.**c** Gene structures of *VvNRT1s*, with UTRs and CDSs shown as green and yellow squares, respectively, and introns are indicated by black lines.

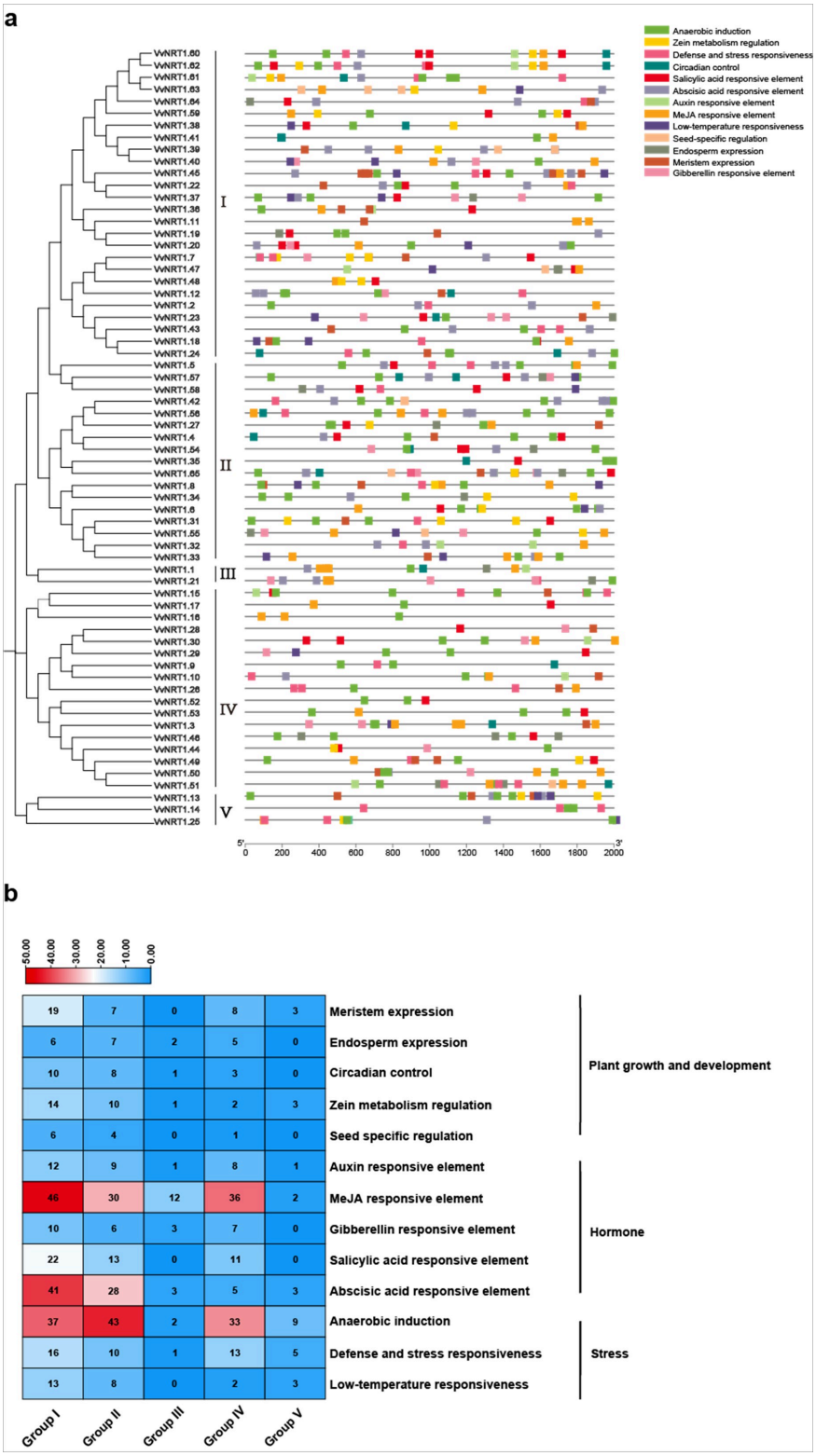


Figure 3

Major cis-acting elements in *VvNRT1* promoters. **a** Location of various cis-element types on chromosomes. Different types of cis-elements are represented by circles of different colors. **b** Heatmap of the abundance of different cis-elements. The red and blue boxes indicate higher and lower numbers of each cis-element type, respectively.

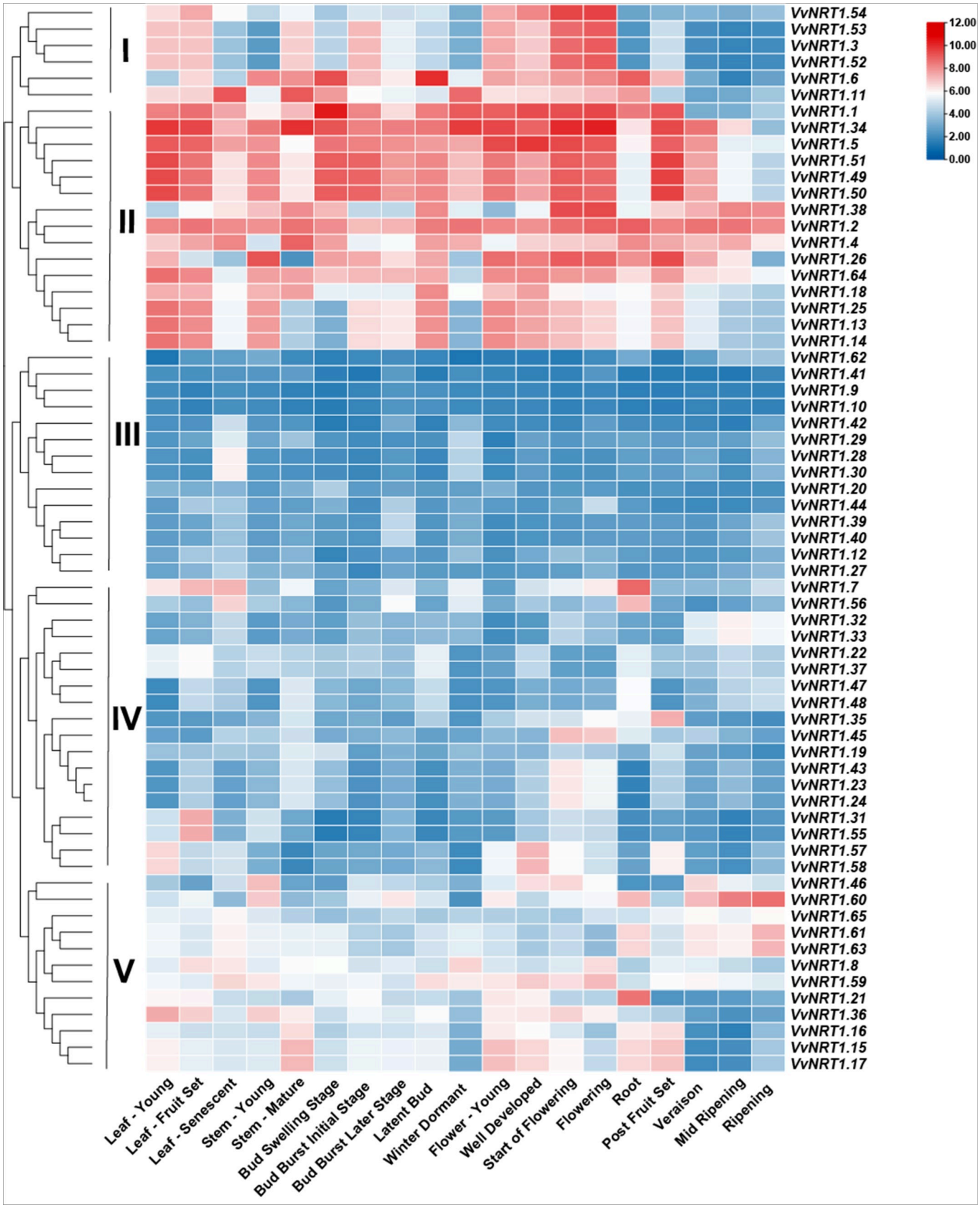


Figure 4

Tissue-specific expression patterns of *VvNRT1* genes**.** The heatmap illustrates the expression profiles of *VvNRT1s* across different grapevine tissues, derived from in silico analysis using data retrieved from the BAR database and mapped to the *Vitis vinifera* T2T2 genome. The expression values were normalized, $\log_2$-transformed, and hierarchically clustered. The color scale from blue to red represents the low to high expression levels of individual *VvNRT1* genes.

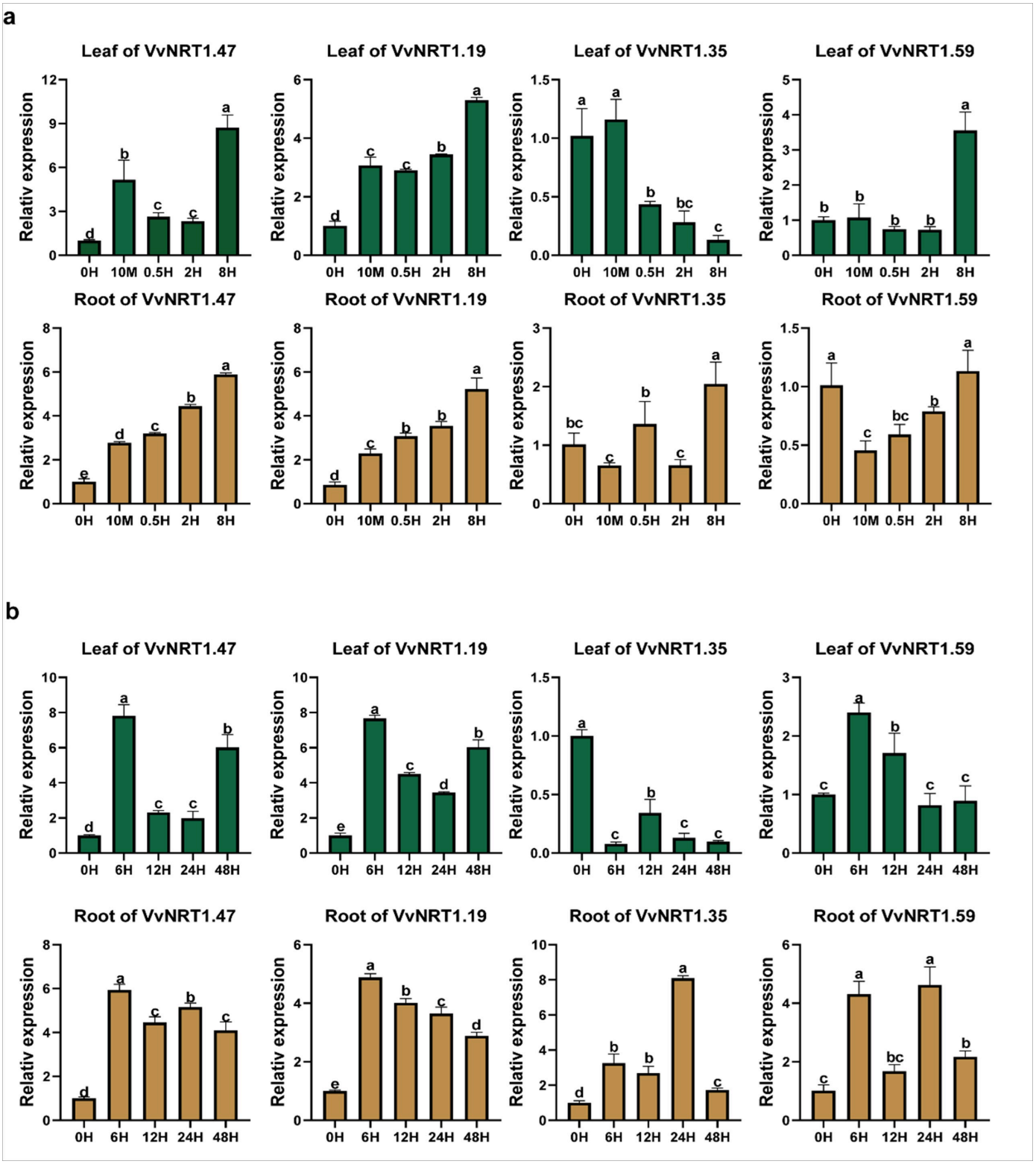


Figure 5

Expression profiles of four *VvNRT1s* in Shine Muscat leaves at various time points after treatment. **a** Expression levels under nitrate treatment. **b** Expression levels following salt treatment. Error bars represent the standard deviation (SD). Different lowercase letters indicate significant differences according to Duncan's multiple range test at $P < 0.05$, whereas identical letters indicate no significant differences. The leaves and roots are highlighted in green and brown, respectively.

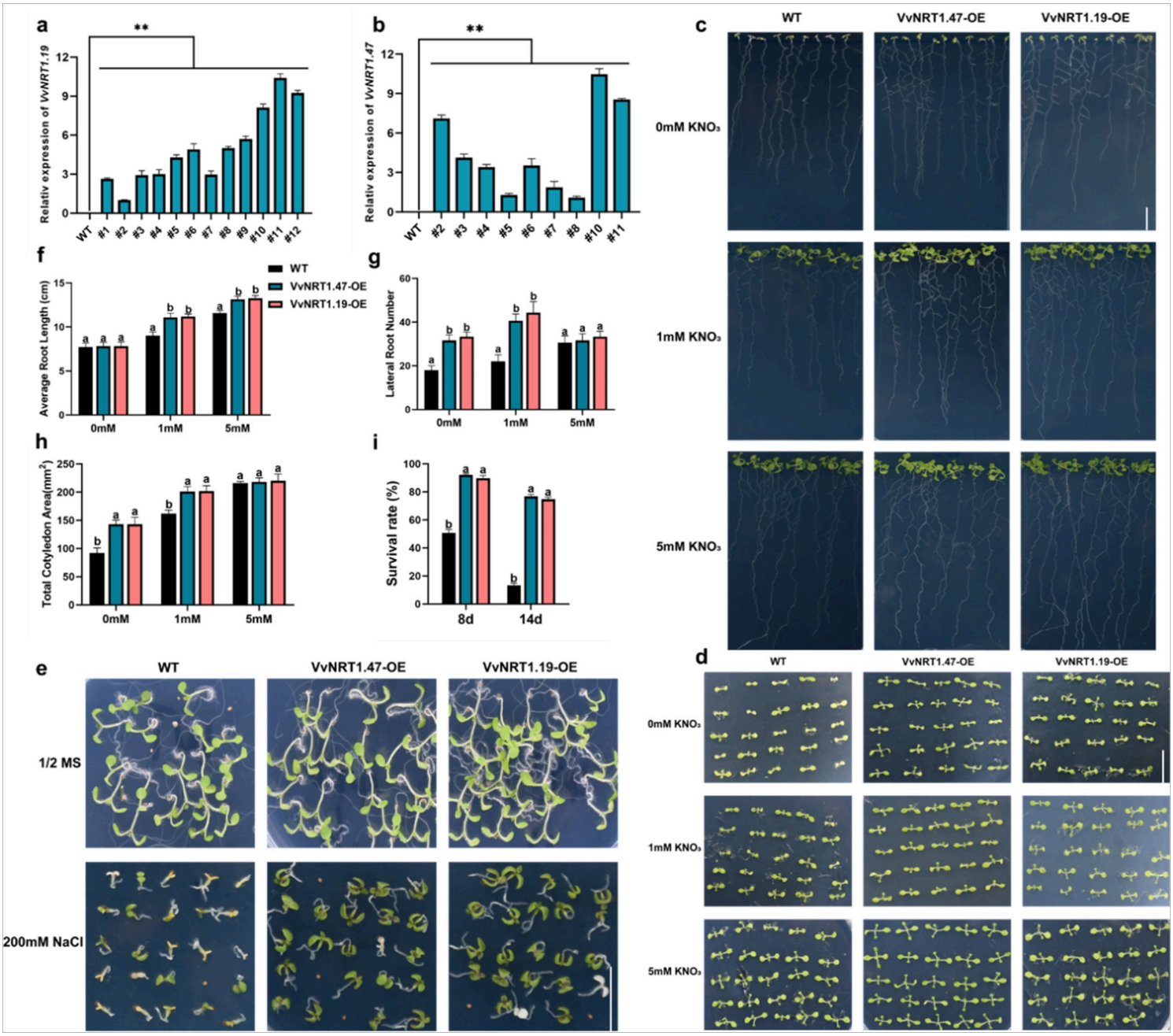


Figure 6

Overexpression of *VvNRT1.19* and *VvNRT1.47* enhances nitrogen utilization and salt tolerance in Arabidopsis. **a** Relative expression levels of *VvNRT1.19* in overexpression (OE) lines and wild-type (WT) plants. **b** Relative expression levels of *VvNRT1.47* in OE lines and WT plants. **c** Root morphology of WT, *VvNRT1.47-OE*, and *VvNRT1.19-OE* seedlings cultivated on half-strength MS (1/2 MS) medium supplemented with 0, 1, or 5 mM KNO_3 as the sole nitrogen source. Scale bar = 1 cm. **d** Whole-seedling phenotypes corresponding to the treatments shown in (c). Scale bar = 1 cm. **e** Phenotypic comparison of WT and transgenic seedlings grown on control (1/2 MS) or salt-stressed medium (1/2 MS + 200 mM NaCl). Scale bar = 1 cm. **f** Mean primary root length of WT and OE lines under different nitrate concentrations (0, 1, and 5 mM KNO_3). **g** Lateral root numbers of WT and OE lines under the same nitrate treatment. **h** Total cotyledon area of WT and OE seedlings grown under varying nitrate concentrations. **i**

Survival rates of WT and OE plants exposed to 200 mM NaCl. Error bars represent the standard deviation (SD). Different lowercase letters indicate statistically significant differences ($P < 0.05$, Student's t-test).